Ultrasonics Sonochemistry 34 (2017) 924–930

Contents lists available at ScienceDirect

Ultrasonics Sonochemistry

journal homepage: www.elsevier.com/locate/ultson

Ultrasound-assisted mineralization of organic contaminants using a recyclable $LaFeO_3$ and Fe^{3+}/persulfate Fenton-like system

S. Ganesh Babu [a], P. Aparna [b], G. Satishkumar [c], Muthupandian Ashokkumar [d], B. Neppolian [a,*]

[a] SRM Research Institute, SRM University, Kattankulathur 603203, Chennai, Tamilnadu, India
[b] Department of Chemistry, Madras Christian College, Tambaram 600059, Chennai, Tamilnadu, India
[c] Department of Chemistry, School of Advanced Sciences, VIT University, Vellore 632014, Tamilnadu, India
[d] School of Chemistry, University of Melbourne, Parkville, VIC 3010, Melbourne, Australia

ARTICLE INFO

Article history:
Received 26 April 2016
Received in revised form 30 July 2016
Accepted 1 August 2016
Available online 1 August 2016

Keywords:
$LaFeO_3$
Ultrasound
4-Chlorophenol
Potassium persulfate
Synergistic effect
Reusable

ABSTRACT

A recyclable heterogeneous catalyst has been successfully developed for application in a Fenton-type advanced oxidation process without adding external H_2O_2. $LaFeO_3$ was prepared from $Fe(NO_3)_3{\cdot}9H_2O$ and $La(NO_3){\cdot}6H_2O$ by a simple sol-gel method and its catalytic efficiency was evaluated for mineralization of 4-chlorophenol using a Fenton-like process. The mineralization process was carried out under ultrasonication in presence of heterogeneous $LaFeO_3$ catalyst with H_2O_2 that was produced during ultrasonication. The mineralization process was monitored through total organic carbon (TOC) analysis. Very importantly, utmost 5-fold synergism was evidenced by the ultrasound mediated $LaFeO_3$-catalyzed system. Besides, more than twofold synergism was observed by combining the ultrasound assisted $LaFeO_3$ catalytic process and potassium persulfate (KPS) assisted advanced oxidation process. It is worth to mention that complete mineralization (~96%) of 4-chlorophenol (initial concentration of 1.25×10^{-4} M) was observed within 1 h in the presence of $LaFeO_3$ (0.5 g L^{-1}) and KPS (1.0 mmol) under ultrasonication (40 kHz). Even after four cycles, the activity of $LaFeO_3$ remained intact which proved its recyclability. Extremely reusable heterogeneous $LaFeO_3$ catalyst makes the system more interesting from both economic and environmental points of view.

1. Introduction

Chemicals are the most common building blocks of various materials used in our day-to-day fundamental needs such as for foods, shelter, medicine, etc. [1]. Owing to the high demand for chemicals in numerous applications, chemical industries process/use chemicals that lead to the discharge of effluents that are toxic mainly because of the aromaticity of compounds such as benzene, toluene, phenol, xylene, etc. [2]. The wastewater from chemical industries requires appropriate treatment before discharging into the environment. Various advanced oxidation processes (AOPs) have been employed for wastewater treatment over the past few decades [3]. Fenton's reagent treatment is one of the most effective technologies for the removal of organic contaminants from industrial and municipal wastewater [4]. Henry John Horstman Fenton firstly reported Fenton's reagent during the 1890's which consists of a homogeneous solution of hydrogen peroxide (H_2O_2) and an iron salt. Both Fenton (Fe^{2+}/H_2O_2) and Fenton-like processes (Fe^{3+}/H_2O_2) produce hydroxyl radical ($HO^{\cdot}$) which is an oxidant that strong enough to degrade organic contaminants present in the wastewater. Complete mineralization of toxic organic contaminants produces H_2O and CO_2 by these Fenton-type oxidation processes. Fenton's reagent exhibits many advantages over other AOPs such as simple operation and low cost [5]. In addition, the operating conditions are generally mild (atmospheric pressure and room temperature) and the excess/remaining H_2O_2 self-decomposes to environmentally safe products [6]. Hence, many research developments were originated based on the Fenton-type oxidation using homogeneous Fe^{2+} or Fe^{3+} salt with hydrogen peroxide. For instance, Ferrer and co-workers demonstrated the ferrous ion-catalyzed Fenton oxidation process for the treatment of extremely polluted industrial wastewater in the presence of H_2O_2 [7]. Similarly, Fenton-type catalyst mediated wet oxidation of methyl *tert*-butyl ether in the presence of H_2O_2 was also demonstrated [8]. Owing to these merits, homogeneous Fenton-type catalysts are widely used to treat industrial wastewater. However, the necessity of higher molar concentrations of ferrous ion and oxidant for each cycle, increase of iron contamination (mostly as iron oxide sludge) after the treatment, and lack of reusability are the major

* Corresponding author.
E-mail address: neppolian.b@res.srmuniv.ac.in (B. Neppolian).

http://dx.doi.org/10.1016/j.ultsonch.2016.08.002
1350-4177/

drawbacks associated with the homogeneous Fenton's reagent oxidation systems [9]. Heterogeneous Fenton-type catalysts lend a hand to overcome these demerits and hence some reusable heterogeneous Fenton-type catalysts were developed recently [10]. Significant contributions were demonstrated for a number of such catalysts including Fe/ZSM-5 for carboxylic acid degradation [11], carbon-Fe catalyst for the degradation of azo dye orange II [12], Fe supported over several materials such as carbon nanotubes, carbon nanofibers, activated carbon, hydrotalcite-like materials, mesoporous silica (MCM-41), silica, silica xerogel, sepiolite, and zeolite USY for the degradation of acid orange II [13], $FeVO_4$ for the degradation of orange II dye [14], and $CoFe_2O_4$ nanocomposites for phenol degradation [15]. Nonetheless, all these catalytic processes were performed only in the presence of H_2O_2.

In recent years, ultrasound assisted Fenton systems find much attention because $H_2O_2/{}^{\cdot}OH$ radicals produced from the sonolysis of water can enhance the Fenton process [16]. For example, Iordache et al. developed a sonoFenton system for the degradation of different pesticides such as 2,4-dichlorophenoxyacetic acid, 4-(2,4-dichlorophenoxy)butyric acid, 4-chloro-o-tolyoxyacetic acid, 3,5-dibromo-4-hidroxybenzonitrile and 3-(4-chlorophenyl)-1,1-di methylurea [17]. Likewise, magnetic Fe_3O_4 was used as a heterogeneous sonoFenton catalyst for the effective degradation of bisphenol A [18]. One of the potential organic pollutants *viz*., pentachlorophenol was degraded by the sono-Fenton system developed based on $Fe@Fe_2O_3$ core-shell nanowires [19]. Some other organic contaminants such as diethyl phthalate, dichlorophenol and Rhodamine B were also degraded by sonoFenton process by different researchers [20–22]. In many of the sonoFenton systems, excess H_2O_2 was added to make the system operational.

Sulfate anion radical $(SO_4^{-\cdot})$, though less selective, is a very reactive and strong oxidizing species, and reacts fast with many organic contaminants. The redox potential of $SO_4^{-\cdot}$ to decompose various pollutants is 2.6 V which is as strong as that of $HO^{\cdot}$ radicals (2.8 V) [8]. For example, the $SO_4^{-\cdot}$ species produced by the photolysis of peroxy disulfate ions $\left(S_2O_8^{2-}\right)$ showed excellent degradation ability which was comparable with that of H_2O_2/UV system for the removal of acetic acid in aqueous solution [23]. Neppolian et al. also proved that ultrasound/persulfate system showed almost similar performance as compared with the coupled ultrasound/homogeneous Fenton $(Fe^{2+})/H_2O_2$ process for the effective degradation of methyl *tert*-butyl ether [8]. In many instances, combination of $HO^{\cdot}$ and $SO_4^{-\cdot}$ radicals ought to exhibit better performances than the individual systems [24]. The results shown herein proved that H_2O_2 produced by the sonolysis of water is strong enough for the mineralization of aromatic organic contaminants (4-chlorophenol was used as a probe) in the presence of a highly reusable heterogeneous $LaFeO_3$ catalyst. Effect of ultrasound on the mineralization of 4-chlorophenol was studied in detail. Interestingly, more than two-fold synergism as well as complete mineralization was obtained by the addition of potassium persulfate (KPS) to this ultrasound assisted heterogeneous process using crystalline perovskite type $LaFeO_3$ catalyst.

2. Experimental section

2.1. Materials and methods

Iron nitrate $[Fe(NO_3)_3{\cdot}9H_2O]$ was purchased from Strem Chemicals, India. Lanthanum nitrate $[La(NO_3){\cdot}6H_2O]$ was procured from Merck Pvt. Ltd. India. Glycine and 4-chlorophenol were obtained from Sigma Aldrich. Milli-Q ultrapure water through Q-POD (Merck Millipore system, conductivity 18.2 MΩ) was used in all experiments. Unless otherwise noted all reactions were carried out at 30 ± 3 °C.

2.2. Preparation of $LaFeO_3$ catalyst

The heterogeneous Fenton's catalyst, $LaFeO_3$ was prepared as described in our previous report [25]. In brief, equal moles (8.86×10^{-3} mol) of iron nitrate $[Fe(NO_3)_3{\cdot}9H_2O]$ and lanthanum nitrate $[La(NO_3){\cdot}6H_2O]$ were dissolved separately in 15 mL of water, then both the solutions were mixed together and stirred for 30 min. To this solution, 0.048 mol of glycine was added and the solution was mixed for another 30 min. Then the solution was evaporated under stirring at 80 °C until gelation occurred. Combustion process was performed in air at 200 °C for 2 h and then calcination was carried out under air flow at 600 °C for 4 h to get $LaFeO_3$ catalyst.

2.3. Reactor set-up, analysis and characterization methods

Mineralization of 4-chlorophenol was carried out in an ultrasonic bath (WENSAR, 40 kHz and 25 L capacity, India). In a typical procedure, 0.5 g L^{-1} of heterogeneous $LaFeO_3$ catalyst was mixed with 4-chlorophenol [100 mL of 1.25×10^{-4} M (9 ppm) solution] and then ultrasonicated over a 40 kHz bath type ultrasonicator with 100% amplitude. The total volume of water in the WENSAR 40 kHz bath type ultrasonicator was maintained at 20 L with 600 W input power for all experiments. The temperature of the bath water was maintained at 30 ± 3 °C. At every 1 h time interval, a desired amount of aliquot was filtered through a syringe filter (0.45 μm nylon membrane syringe filter) to remove the residual $LaFeO_3$. The filtered samples were immediately analyzed through total organic carbon (TOC) analyzer (Shimadzu TOC-L instrument, Japan). Low frequency ultra-sonic horn operating at 20 kHz from SONICS, Vibra cell, USA was used for the probe type mineralization studies. A 13 mm diameter high intensity probe was used in this instrument and the system was maintained at a constant temperature (30 ± 2 °C) throughout the process with a water circulation jacket.

To investigate the crystal structure of $LaFeO_3$ catalyst, powder XRD studies were carried out using PANaltical X'pert powder diffractometer using Cu Kα radiation. Perkin Elmer, USA Fourier Transform Infrared spectroscopy was used for FT-IR analysis. The surface morphology and elemental analysis were determined by means of SEM-EDS analysis recorded using FEI Quanta FEG 200 HR-SEM instrument operated at 20 kV. Tecnai G2 transmission electron microscope was operated at 200 kV to do the TEM analysis of $LaFeO_3$ catalyst. BET surface area, pore area and pore volume analyses were performed using micromeritics TriStar II 3020 instrument. The $LaFeO_3$ catalyst was de-gassed at 150 °C under vacuum before the adsorption of nitrogen.

3. Results and discussion

3.1. Catalyst characterization

Formation of $LaFeO_3$ catalyst and its chemical composition and crystal structure were evaluated by powder XRD analysis. The XRD pattern of prepared $LaFeO_3$ catalyst is shown in Fig. 1(a). All the peaks of XRD pattern match with the JCPDS data (JCPDS # 74-2203) [26]. The sharp intense XRD peaks are attributed to the well crystalline perovskite type $LaFeO_3$ obtained by calcination of the sample at 600 °C. However, no additional XRD peaks corresponding to La_2O_3, Fe_2O_3 or other crystalline impurities were detected which confirmed the formation of single phase $LaFeO_3$. The FT-IR spectrum of the as-prepared $LaFeO_3$ is shown in Fig. 1(b). The peak at 3439 cm^{-1} is due to the bending vibration of O–H from surface absorbed water or hydroxyl group. The band at 2923 cm^{-1} corresponds to absorbed atmospheric CO_2 resulting from the

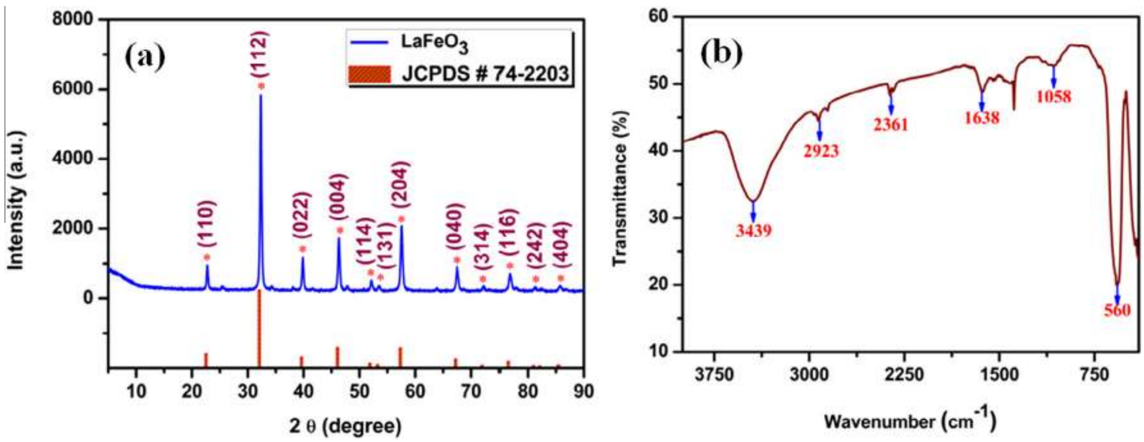

Fig. 1. (a) Powder XRD pattern and (b) FT-IR spectrum of $LaFeO_3$ catalyst.

preparation and processing of the FTIR sample in an ambient atmosphere. The bands at 2361 and 1638 cm^{-1} are attributed to the symmetric and asymmetric stretching of the carboxyl group, respectively. The principle vibration of CO_3^{2-} is observed as a less intense band at 1058 cm^{-1} which authenticated the presence of La-carbonate species present at the surface of $LaFeO_3$ catalyst which was not detected in XRD [27]. The Fe–O stretching vibration of octahedral FeO_6 group of $LaFeO_3$ contributed to the well intense band at 560 cm^{-1} in the spectrum [28].

To find the surface morphology of $LaFeO_3$ catalyst, SEM analysis was carried out. The FE-SEM images and EDS spectrum are depicted in Fig. 2(a–c). Wafer-like morphology of $LaFeO_3$ is clearly evident in higher magnification SEM images. No separate iron oxide moieties were identified in the SEM images which revealed that Fe ions are present within the unit cells. This kind of arrangement increases the stability of the $LaFeO_3$ catalyst. The EDS spectrum exhibited the presence of La, Fe and O elements and confirmed the purity of as-prepared catalyst. The morphology of $LaFeO_3$ catalyst was further analyzed by TEM analysis. The TEM micrographs are given in Fig. 3(a–c). The TEM images confirmed the irregular layered shape of $LaFeO_3$ catalyst. The lattice fringes are clearly visible in the high magnification (10 nm scale bar) TEM image which is illustrated in Fig. 3(c). The surface area of the as-prepared $LaFeO_3$ catalyst was found to be 9.91 m^2/g as determined by BET analysis based on the N_2 adsorption-desorption studies. As can be seen from Fig. 4, $LaFeO_3$ catalyst represented a type IV isotherm characteristic of mesoporous material. The pore size and pore volume were found to be 274.3 Å and 0.068 cm^3/g, respectively.

3.2. Catalytic mineralization of 4-chlorophenol

Sonolysis of water generates $HO^{\cdot}$ and $H^{\cdot}$ radicals by the hemolytic cleavage of H_2O (Reaction (1)) [29]. A part of $HO^{\cdot}$ radicals combine to form hydrogen peroxide (H_2O_2) (Reaction (2)). H_2O_2 reacts with $LaFeO_3$ catalyst (with Fe^{3+} ion) to generate $HOO^{\cdot}$ radical and H^+ ion (Reaction (3)). Fe^{2+} ions were oxidized to Fe^{3+} by H_2O_2 (Reaction (4)). As a result of this process, $HO^{\cdot}$ radical and OH^- ion were produced as by-products. Further reduction of Fe^{3+} ion was also carried out by means of $HOO^{\cdot}$ and $OO^{-\cdot}$ species as shown in Reactions (5) and (6). The $HO^{\cdot}$ radical produced by the sonolysis of water reacts with H_2O_2 to form $HOO^{\cdot}$ and H_2O (Reaction (7)) [30]. The $HO^{\cdot}$ and $HOO^{\cdot}$ radicals involved in the mineralization of 4-chlorophenol. Finally, the mineralization of 4-chlorophenol by this sonoFenton process-catalyzed by perovskite type $LaFeO_3$ catalyst yielded CO_2 and H_2O (Reaction (8)).

$$H_2O +)))) \text{ (ultrasound)} \rightarrow HO^{\cdot} + H^{\cdot} \quad (1)$$

$$HO^{\cdot} + HO^{\cdot} \rightarrow H_2O_2 \quad (2)$$

$$Fe^{3+} + H_2O_2 \rightarrow Fe^{2+} + HOO^{\cdot} + H^+ \quad (3)$$

$$Fe^{2+} + H_2O_2 \rightarrow Fe^{3+} + HO^{\cdot} + OH^- \quad (4)$$

$$Fe^{3+} + HOO^{\cdot} \rightarrow Fe^{2+} + OO^{-\cdot} + H^+ \quad (5)$$

$$Fe^{3+} + OO^{-\cdot} \rightarrow Fe^{2+} + O_2 \quad (6)$$

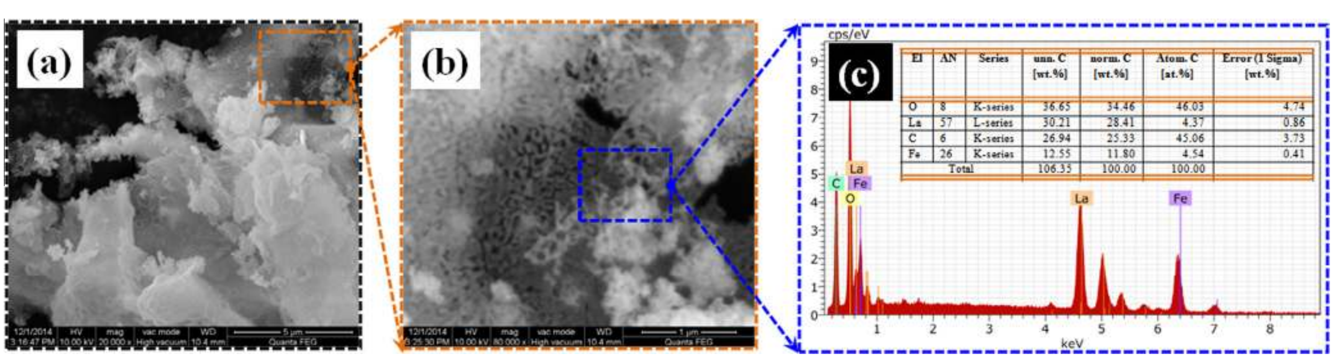

Fig. 2. (a and b) SEM images and (c) the corresponding EDS spectrum of $LaFeO_3$ catalyst [inset: wt% table].

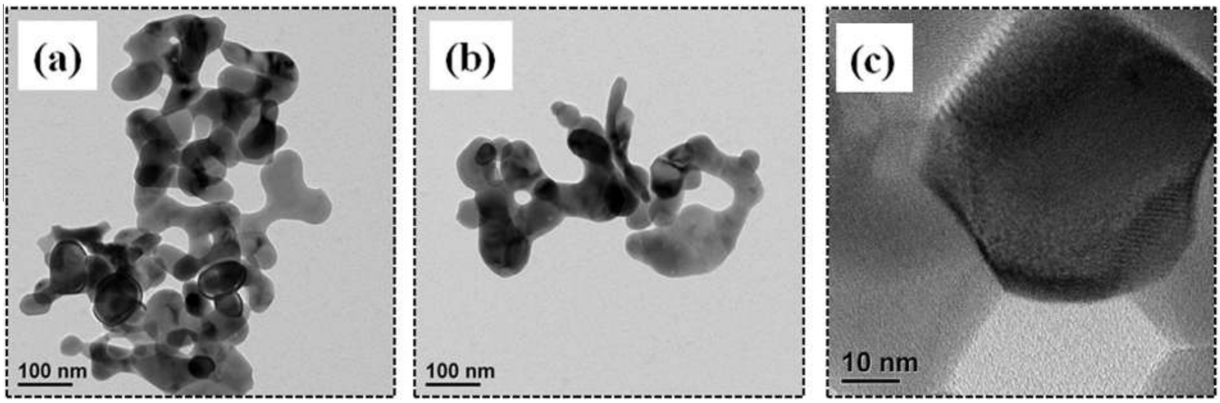

Fig. 3. TEM images of $LaFeO_3$ catalyst with different magnification (a and b) 100 nm and (c) 10 nm bar scales.

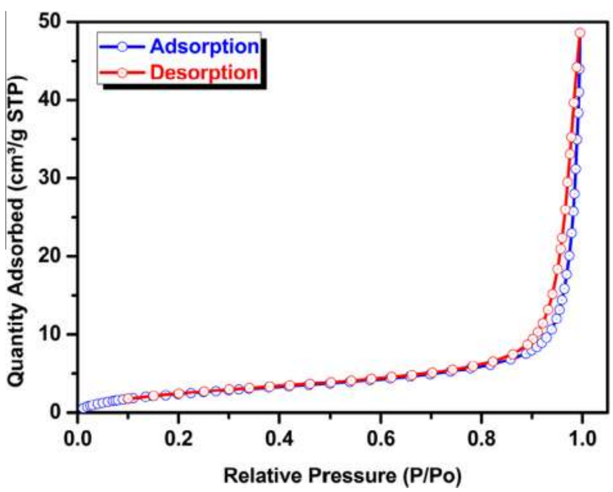

Fig. 4. N_2-adsorption/desorption isotherm of $LaFeO_3$ catalyst.

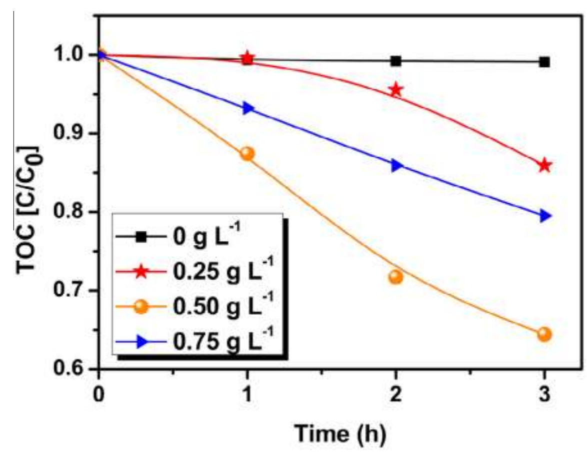

Fig. 5. Effect of catalyst dosage [Experimental conditions: $LaFeO_3$ and 4-chlorophenol (1.25×10^{-4} M) were ultrasonicated (40 kHz) for 3 h].

$$HO^{\cdot} + H_2O_2 \rightarrow HOO^{\cdot} + H_2O \quad (7)$$

$$p\text{-Cl—}C_6H_4\text{—OH} + HO^{\cdot} \text{ and/or } HOO^{\cdot} \rightarrow CO_2 + H_2O \quad (8)$$

In order to find optimal experimental conditions for the mineralization of organic pollutants, reaction parameters such as catalyst dosage, initial concentration of 4-chlorophenol, amplitude of ultrasound and amount of potassium persulfate (an oxidizing agent) on mineralization rate were varied.

3.2.1. Effect of catalyst dosage

Catalyst dosage is a very important factor capable of altering the rate of mineralization reaction considerably [31–34]. Therefore, the effect of catalyst dosage on the ultrasound-assisted mineralization of 4-chlorophenol was studied initially. For this purpose, a series of experiments were carried out by varying the catalyst ($LaFeO_3$) dosage from 0 to 0.75 g L^{-1} under ultrasonication (40 kHz) (Fig. 5). As evident from Fig. 5, no mineralization was observed without addition of $LaFeO_3$ catalyst. However, with an increase in catalyst amount to 0.25 and 0.5 g L^{-1}, the mineralization efficiency increased to about 15% and 35%, after 3 h, respectively. Further increase in catalyst dosage to 0.75 g L^{-1} caused a decrement in mineralization of 4-chlorophenol, (20%). This can be well explained by the fact that the higher concentration of $LaFeO_3$ could lead to the scavenging of $^{\cdot}OH$ radicals by excess iron ions which caused a decrease in mineralization rate [35]. From the experimental results, the optimized dosage of $LaFeO_3$ was found to be 0.5 g L^{-1} for 1.25×10^{-4} M 4-chlorophenol solution. Thus, 0.5 g L^{-1} of $LaFeO_3$ catalyst loading was used for further studies.

3.2.2. Effect of initial concentration of 4-chlorophenol

The mineralization efficiency of $LaFeO_3$ catalyst as a function of initial concentration of 4-chlorophenol was investigated. For this purpose, a series of experiments were carried out with different initial concentrations of 4-chlorophenol (0.625×10^{-4} to 3.75×10^{-4} M) (Fig. 6). It is clearly evident from the Fig. 6 that the percentage mineralization was maximum at all the time with 1.25×10^{-4} M of 4-chlorophenol. The overall mineralization efficiency increases with an increase in the initial concentration and a maximum is reached at 1.25×10^{-4} M concentration of 4-chlorophenol. However, the higher concentrated 4-chlorophenol was not completely degraded in the presence of 0.5 g L^{-1} of $LaFeO_3$ catalyst which might be due to inadequate hydroxyl radicals produced under the reaction conditions used. In order to support this observation, the amount of H_2O_2 produced in the bath type sonicator over a period of time was measured. The estimated H_2O_2 concentrations were 0.0066, 0.0091 and 0.0102 mmol at 1, 2 and 3 h, respectively. A similar result was observed by Hu and co-workers for the photo-Fenton degradation of acid black 1 (AB1) in which the degradation was higher at lower concentration of AB1 [36].

3.2.3. Effect of ultrasound

To understand the effect of ultrasound on the mineralization of 4-chlorophnol (1.25×10^{-4} M), three experiments were carried

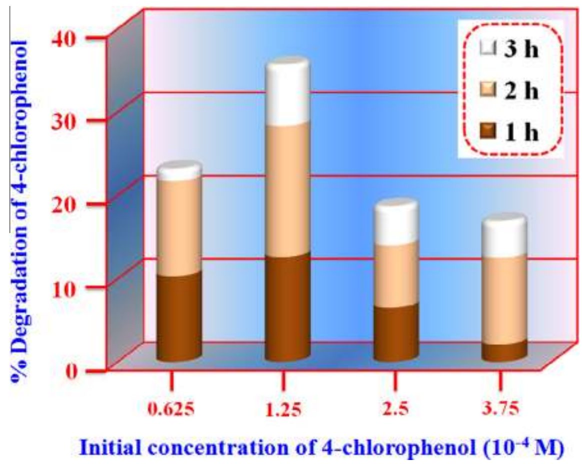

Fig. 6. Effect of initial concentration of 4-chlorophenol [Experimental conditions: $LaFeO_3$ (0.5 g L^{-1}) and 4-chlorophenol were ultrasonicated (40 kHz) for 3 h].

out under different reaction cirucumstances. As can be seen from Fig. 7, no mineralization of 4-chlorophnol (1.25×10^{-4} M) was found under ultrasonication (sonolysis) alone. Likewise, significant mineralization of 4-chlorophnol was not observed when stirred with $LaFeO_3$ catalyst (0.5 g L^{-1}) (catalysis) alone. However, the combination of ultrasound-assisted mineralization technique with Fenton-like $LaFeO_3$ catalytic system (sonocatalysis) showed improved mineralization efficiency. The synergism was calculated based on the Eq. (9) and an utmost synergism of 5.3 was experienced by this combinatorial system. A similar synergism was observed by Neppolian et al. for the Fenton-like oxidation on enhanced oxidative mineralization of *para*-chlorobenzoic acid by ultrasonic irradiation [4]. It is worth to mention here is that this tremendous synergistic effect makes the present system more favourable in the environmental points of view.

$$\text{Synergistic effect} = \frac{[\%TOC]_{sonocatalysis}}{[\%TOC]_{sonolysis} + [\%TOC]_{catalysis}} \tag{9}$$

3.2.4. Effect of sonoreactor type

To investigate the effect of sonoreactor type on the mineralization of 4-chlorophnol (1.25×10^{-4} M), two experiments were performed with different ultrasonicators such as 20 kHz (probe type) and 40 kHz (bath type) in presence of $LaFeO_3$ catalyst (0.5 g L^{-1}) for the mineralization of 4-chlorophenol solution and the results are depicted in Fig. 8. The results emphasized that more or less equal amount of mineralization was observed with 20 kHz and 40 kHz ultrasonicators in the presence of 0.5 g L^{-1} of $LaFeO_3$ catalyst. A similar effect was observed by Price and co-workers for the ultrasound assisted Fenton-type process in the mineralization of Reactive Blue 19 [37]. It is a well known fact that the concentration of H_2O_2 played a vital role in the mineralization of organic pollutant. Both the lower frequency ultrasonicators (20 kHz and 40 kHz) produced most optimal amount of H_2O_2 that enhanced the mineralization of 4-chlorophenol in the presence of $LaFeO_3$ catalyst. To acquire a clear vision about the formation of H_2O_2, the amount of H_2O_2 produced from these two reactors were quantified and given in the inset of Fig. 8. It is clearly evidenced from the H_2O_2 estimation that the concentration of H_2O_2 is exponentially increased with respect to the sonication time. Nonetheless, change in ultrasonication process (either probe type or bath type ultrasonicators) exhibited no significant influence in the rate of mineralization of 4-chlorophenol.

3.2.5. Effect of potassium persulfate

In order to facilitate the mineralization efficiency of $LaFeO_3$ catalyst, ultrasound assisted mineralization was performed by adding a small amount of potassium persulfate (KPS). Besides, the effect of initial concentration of KPS was also investigated (Fig. 9). The results reveal that 3 h of ultrasonication was required for almost complete mineralization of 4-chlorophenol (1.25×10^{-4} M) with 0.5 mmol KPS, whereas with 1.0 mmol KPS, ~97% mineralization was achieved at 1 h of reaction time. Based on the observation and previous literature reports, a possible reaction pathway is proposed for the mineralization of 4-chlorophenol using ultrasound induced KPS [Reactions (10)–(12)] [38].

$$S_2O_8^{2-} + \text{heat and })))) \rightarrow 2SO_4^{-\cdot} \tag{10}$$

$$2SO_4^{-\cdot} + H_2O \rightarrow HO^{\cdot} + H^+ + SO_4^{2-} \tag{11}$$

$$P\text{-Cl—}C_6H_4\text{—OH} + HO^{\cdot} \rightarrow CO_2 + H_2O \tag{12}$$

More interestingly ca. twofold increase was observed by combining ultrasound assisted $LaFeO_3$ catalytic process and KPS for the mineralization of 4-chlorophenol under ambient reaction conditions. The synergy was calculated based on Eq. (13) and the results are given in Table 1. It is noteworthy to mention here that

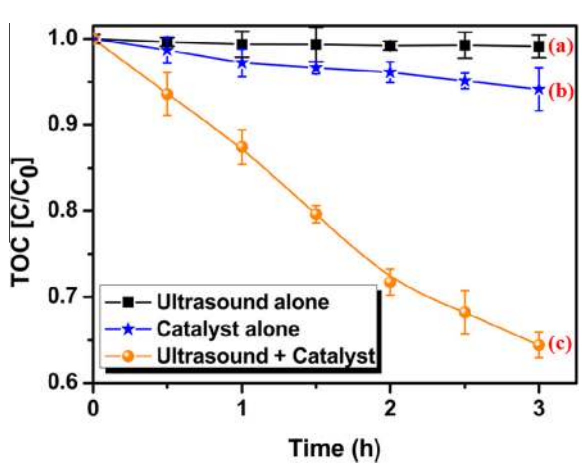

Fig. 7. TOC as a function of time [Experimental conditions: (a) 4-chlorophenol (1.25×10^{-4} M) were ultrasonicated (40 kHz) for 3 h, (b) $LaFeO_3$ (0.5 g L^{-1}) stirred with 4-chlorophenol (1.25×10^{-4} M) for 3 h and (c) $LaFeO_3$ (0.5 g L^{-1}) and 4-chlorophenol (1.25×10^{-4} M) were ultrasonicated (40 kHz) for 3 h].

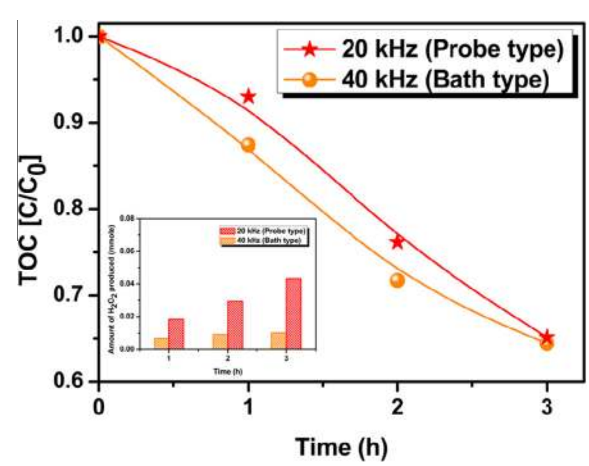

Fig. 8. Effect of ultrasound frequency [Experimental conditions: $LaFeO_3$ (0.5 g L^{-1}) and 4-chlorophenol (1.25×10^{-4} M) were ultrasonicated (20 kHz or 40 kHz) for 3 h] [inset: amount of H_2O_2 (mmol) produced from each sonicator].

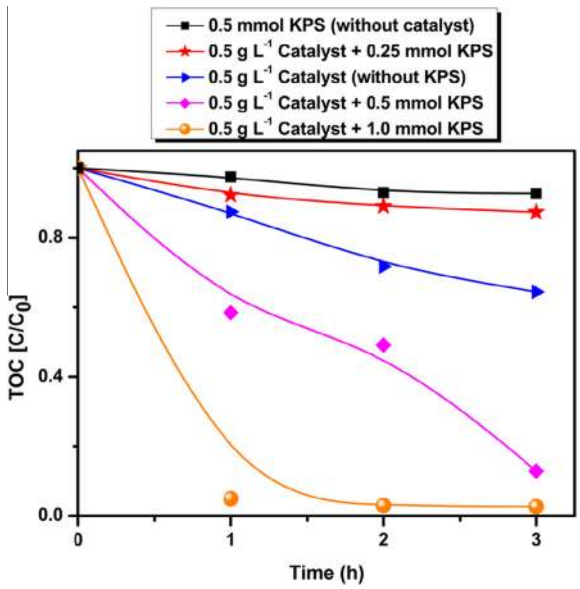

Fig. 9. Effect of potassium persulfate (KPS) [Experimental conditions: $LaFeO_3$ ($0.5\ g\ L^{-1}$), 4-chlorophenol (1.25×10^{-4} M) and KPS were ultrasonicated (40 kHz) for 3 h].

the combined effect of HO˙ radicals produced by KPS under ultrasonication and HO˙ as well as HOO˙ radicals generated by the ultrasound assisted $LaFeO_3$ sonocatalytic process are the main reason for this highest synergism. Besides, the mineralization of 4-chlorophenol was relatively slowed down after 2 h of ultrasonication either with $LaFeO_3$ alone or with KPS alone. To evidence this, only 5.3% and 0.2% TOC removal was observed with $LaFeO_3$ alone and with KPS alone, respectively after 2 h. At the same time, the combinatorial system ($LaFeO_3$ and KPS) progressed gradually even after 2 h and the complete mineralization was achieved at 3 h. This set of experiments clearly proved that the present ultrasound assisted combined system ($LaFeO_3$ and KPS) not only resulted in high synergism but also led to complete mineralization (almost 100% mineralization).

$$\text{Synergistic effect} = \frac{[\%\text{TOC}]_{\text{catalyst+KPS}}}{[\%\text{TOC}]_{\text{catalyst}} + [\%\text{TOC}]_{\text{KPS}}} \qquad (13)$$

3.2.6. Recyclability test

Reusability of the catalyst is one of the most important characteristics, especially for the heterogeneous catalytic systems [39–41]. In the present system, $LaFeO_3$ catalyst was easily separated from the reaction mixture after the completion of the reaction by centrifugation. The recovered catalyst was washed with water and dried at 60 °C for 2 h. Then, it was well dispersed in fresh 4-chlorophenol (1.25×10^{-4} M) solution under ultrasonication and KPS (0.5 mmol) were added to the reaction mixture to test recyclability of the catalyst. The reactivity of $LaFeO_3$ catalyst remained intact even up to four consecutive experiments under identical reaction conditions (Fig. 10). In all the four reaction cycles, ~90% of the total organic carbon was removed from the solution in 3 h. This result implied the remarkable stability of the $LaFeO_3$ catalyst.

Table 1
Synergistic effect of ultrasound assisted $LaFeO_3$ and KPS system for the mineralization of 4-chlorophenol.[a]

Entry	Reaction time (h)	TOC removal (%)			Synergy
		$LaFeO_3$ ($0.5\ g\ L^{-1}$)	KPS (0.5 mmol)	$LaFeO_3$ ($0.5\ g\ L^{-1}$) + KPS (0.5 mmol)	
1	1	12.5	2.5	32.1	2.1
	2	30.3	7.0	65.4	1.7
	3	35.6	7.2	90.2	2.1

[a] $LaFeO_3$ ($0.5\ g\ L^{-1}$), KPS (0.5 mmol) and 4-chlorophenol (1.25×10^{-4} M) were ultrasonicated (40 kHz) for 3 h.

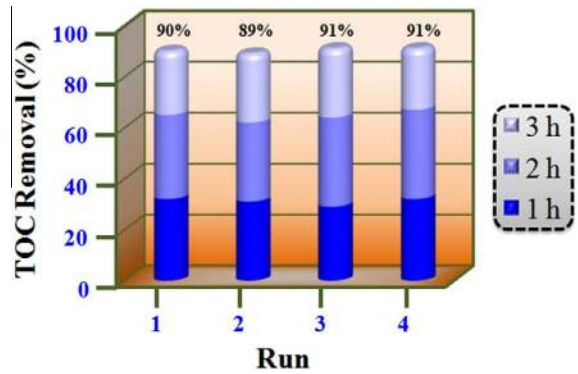

Fig. 10. Recyclability test [Experimental conditions: $LaFeO_3$ ($0.5\ g\ L^{-1}$), 4-chlorophenol (1.25×10^{-4} M) and KPS (0.5 mmol) were ultrasonicated (40 kHz) for 3 h].

4. Conclusions

Reusable heterogeneous Fenton-type $LaFeO_3$ catalyst was prepared by sol-gel method and used for the mineralization of 4-chlorophenol under ultrasonication. The influence of catalyst dosage and initial concentration of 4-chlorophenol were tested. It is worth to mention here that more than fivefold synergism was experienced by combining the sono-degradation and Fenton degradation techniques without adding external H_2O_2. Effect of ultrasonication type (probe and bath) was examined and proven to be similar in performance against the mineralization of 4-chlorophenol. The addition of a small amount of KPS substantially enhanced the mineralization rate. Besides, more than twofold increase in the rate of degradation with a synergy index >2 were observed by the addition of small amount of KPS to the reaction mixture. Additionally, $LaFeO_3$ catalyst was recycled for four times without any decrease in reactivity for the mineralization of 4-chlorophenol. Highly reusable heterogeneous perovskite type $LaFeO_3$ catalyst, high synergistic effect due to the ultrasound and complete mineralization by the addition of KPS make this system economically and environmentally feasible.

Acknowledgement

This work was supported by Science and Engineering Research Board-Department of Science and Technology (SERB-DST), New Delhi, India [File No.: EMR/2014/000645].

References

[1] B. Kamm, Production of platform chemicals and synthesis gas from biomass, Angew. Chem. Int. Ed. 46 (2007) 5056–5058.
[2] S.R. Kanel, B. Neppolian, H. Choi, J.W. Yang, Heterogeneous catalytic oxidation of phenanthrene by hydrogen peroxide in soil slurry: kinetics, mechanism, and implication, Soil Sediment. Contam. 12 (2003) 101–117.
[3] M. Gopiraman, S.G. Babu, Z. Khatri, B.S. Kim, K. Wei, R. Karvembu, I.S. Kim, Photodegradation of dyes by a novel TiO_2/u-RuO_2/GNS nanocatalyst derived from Ru/GNS after its use as catalyst in aerial oxidation of primary alcohols (GNS = graphene nanosheets), React. Kinet. Mech. Catal. 115 (2015) 759–772.
[4] B. Neppolian, J.-S. Park, H. Choi, Effect of Fenton-like oxidation on enhanced oxidative degradation of para-chlorobenzoic acid by ultrasonic irradiation, Ultrason. Sonochem. 11 (2004) 273–279.

[5] S.M. Arnold, W.J. Hickey, R.F. Harris, Degradation of atrazine by Fenton's reagent: condition optimization and product quantification, Environ. Sci. Technol. 29 (1995) 2083–2089.

[6] J.A. Zazo, J.A. Casas, A.F. Mohedano, J.J. Rodriguez, Catalytic wet peroxide oxidation of phenol with a Fe/active carbon catalyst, Appl. Catal. B: Environ. 65 (2006) 261–268.

[7] N.S.S. Martinez, J.F. Fernandez, X.F. Segura, A.S. Ferrer, Pre-oxidation of an extremely polluted industrial wastewater by the Fenton's reagent, J. Hazard. Mater. 101 (2003) 315–322.

[8] B. Neppolian, H. Jung, H. Choi, J.H. Lee, J.-W. Kang, Sonolytic degradation of methyl *tert*-butyl ether: the role of coupled Fenton process and persulphate ion, Water Res. 36 (2002) 4699–4708.

[9] C.A. Tolman, W. Tumas, S.Y.L. Lee, D. Campos, in: D.H.R. Barton (Ed.), The Activation of Dioxygen and Homogeneous Catalytic Oxidation, Plenum Press, New York, 1993, p. 57.

[10] E.G.G. Ramirez, B.K.G. Theng, M.L. Mora, Clays and oxide minerals as catalysts and nanocatalysts in Fenton-like reactions – a review, Appl. Clay Sci. 47 (2010) 182–192.

[11] G. Centi, S. Perathoner, T. Torre, M.G. Verduna, Catalytic wet oxidation with H_2O_2 of carboxylic acids on homogeneous and heterogeneous Fenton-type catalysts, Catal. Today 55 (2000) 61–69.

[12] J.H. Ramirez, F.J.M. Hodar, A.F.P. Cadenas, C.M. Castilla, C.A. Costa, L.M. Madeira, Azo-dye Orange II degradation by heterogeneous Fenton-like reaction using carbon-Fe catalysts, Appl. Catal. B: Environ. 75 (2007) 312–323.

[13] A. Rodriguez, G. Ovejero, J.L. Sotelo, M. Mestanza, J. Garcia, Heterogeneous Fenton catalyst supports screening for mono azo dye degradation in contaminated wastewaters, Ind. Eng. Chem. Res. 49 (2010) 498–505.

[14] J. Deng, J. Jiang, Y. Zhang, X. Lin, C. Du, Y. Xiong, $FeVO_4$ as a highly active heterogeneous Fenton-like catalyst towards the degradation of Orange II, Appl. Catal. B: Environ. 84 (2008) 468–473.

[15] F.-X. Qin, S.-Y. Jia, Y. Liu, X. Han, H.-T. Ren, W.-W. Zhang, J.-W. Hou, S.-H. Wu, Metal-organic framework as a template for synthesis of magnetic $CoFe_2O_4$ nanocomposites for phenol degradation, Mater. Lett. 101 (2013) 93–95.

[16] M.A. Beckett, I. Hua, Enhanced sonochemical decomposition of 1,4-dioxane by ferrous iron, Water Res. 37 (2003) 2372–2376.

[17] I. Iordache, S. Wilson, E. Lundanes, M. Iordache, V.L. Pave, N. Aelenei, The Fenton and sono-Fenton processes applied for pesticide degradation, Environ. Eng. Manage. J. 9 (2010) 519–525.

[18] R. Huang, Z. Fang, X. Yan, W. Cheng, Heterogeneous sono-Fenton catalytic degradation of bisphenol A by Fe_3O_4 magnetic nanoparticles under neutral condition, Chem. Eng. J. 197 (2012) 242–249.

[19] T. Luo, Z. Ai, L. Zhang, Fe@Fe_2O_3 core-shell nanowires as iron reagent. 4. Sono-Fenton degradation of pentachlorophenol and the mechanism analysis, J. Phys. Chem. C 112 (2008) 8675–8681.

[20] A. Hwang, S. Na, J. Ha, J. Khim, Degradation of diethyl phthalate by sono-Fenton process and its dependence on the power density, Jpn. J. Appl. Phys. 50 (2011) 7–9.

[21] P.J.D. Ranjit, K. Palanivelu, C.-S. Lee, Degradation of 2,4-dichlorophenol in aqueous solution by sono-Fenton method, Korean J. Chem. Eng. 25 (2008) 112–117.

[22] Z. Ai, L. Lu, J. Li, L. Zhang, J. Qiu, M. Wu, Fe@Fe_2O_3 core-shell nanowires as iron reagent efficient degradation of rhodamine B by a novel sono-Fenton process, J. Phys. Chem. C 111 (2007) 4087–4093.

[23] J. Criquet, N.K.V. Leitner, Degradation of acetic acid with sulfate radical generated by persulfate ions photolysis, Chemosphere 77 (2009) 194–200.

[24] G.P. Anipsitakis, D.D. Dionysiou, Degradation of organic contaminants in water with sulfate radicals generated by the conjunction of peroxymonosulfate with cobalt, Environ. Sci. Technol. 37 (2003) 4790–4797.

[25] G. Satishkumar, M.V. Landau, T. Buzaglo, L. Frimet, M. Ferentz, R. Vidruk, F. Wagner, Y. Gal, M. Herskowitz, Fe/SiO_2 heterogeneous Fenton catalyst for continuous catalytic wet peroxide oxidation prepared in situ by grafting of iron released from $LaFeO_3$, Appl. Catal. B: Environ. 138–139 (2013) 276–284.

[26] S. Thirumalairajan, K. Girija, V.R. Mastelaro, V. Ganesh, N. Ponpandian, Detection of the neurotransmitter dopamine by a glassy carbon electrode modified with self-assembled perovskite $LaFeO_3$ microspheres made up of nanospheres, RSC Adv. 4 (2014) 25957–25962.

[27] S. Thirumalairajan, K. Girija, V.R. Mastelaro, N. Ponpandian, Photocatalytic degradation of organic dyes under visible light irradiation by floral-like $LaFeO_3$ nanostructures comprised of nanosheet petals, New J. Chem. 38 (2014) 5480–5490.

[28] Z.X. Wei, Y.H. Xu, H.Y. Liu, C.H. Hu, Preparation and catalytic activities of $LaFeO_3$ and Fe_2O_3 for HMX thermal decomposition, J. Hazard. Mater. 165 (2009) 1056–1061.

[29] M. Korn, M.V.A.S. Andrade, S.S. Borges, C.S. Sousa, F.S. Oliveir, Reagent generation assisted by ultrasonic irradiation, J. Braz. Chem. Soc. 14 (2003) 254–258.

[30] M.B. Kasiri, H. Aleboyeh, A. Aleboyeh, Degradation of Acid Blue 74 using Fe-ZSM5 zeolite as a heterogeneous photo-Fenton catalyst, Appl. Catal. B: Environ. 84 (2008) 9–15.

[31] P. Karthik, R. Vinoth, S.G. Babu, M. Wen, T. Kamegawa, H. Yamashita, B. Neppolian, Synthesis of highly visible light active TiO_2-2-Naphthol surface complex and its application in photocatalytic chromium (VI) reduction, RSC Adv. 5 (2015) 39752–39759.

[32] P.S. Kumar, M. Selvakumar, S.G. Babu, S. Jaganathan, S. Karuthapandian, Novel CuO/Chitosan nanocomposite thin film: facile hand picking recoverable, efficient and reusable heterogeneous photocatalyst, RSC Adv. 5 (2015) 57493–57501.

[33] P.S. Kumar, M. Selvakumar, S.G. Babu, S. Karuthapandian, S. Chattopadhyay, CdO nanospheres: facile synthesis and band gap modification for the superior photocatalytic activity, Mater. Lett. 151 (2015) 45–48.

[34] S.G. Babu, A.S. Vijayan, B. Neppolian, SnS_2/rGO: an efficient photocatalyst for the complete degradation of organic contaminants, Mater. Focus 4 (2015) 272–276.

[35] H. Xu, M. Li, H. Wang, J. Miao, L. Zou, Fenton reagent oxidation and decolorizing reaction kinetics of reactive red SBE, Energy Proc. 16 (2012) 58–64.

[36] A.C.-K. Yip, F.L.-Y. Lam, X. Hu, Chemical-vapor-deposited copper on acid-activated bentonite clay as an applicable heterogeneous catalyst for the photo-Fenton-like oxidation of textile organic pollutants, Ind. Eng. Chem. Res. 44 (2005) 7983–7990.

[37] M. Siddique, R. Farooq, G.J. Price, Synergistic effects of combining ultrasound with the Fenton process in the degradation of reactive blue 19, Ultrason. Sonochem. 21 (2014) 1206–1212.

[38] B. Neppolian, E. Celik, H. Choi, Photochemical oxidation of arsenic(III) to arsenic(V) using peroxy disulfate ions as an oxidizing agent, Environ. Sci. Technol. 42 (2008) 6179–6184.

[39] S.G. Babu, R. Vinoth, B. Neppolian, D.D. Dionysiou, M. Ashokkumar, Diffused sunlight-driven highly synergistic pathway for complete mineralization of organic contaminants using reduced graphene oxide supported photocatalyst, J. Hazard. Mater. 291 (2015) 83–92.

[40] S.G. Babu, R. Vinoth, D.P. Kumar, M.V. Shankar, H.L. Chou, K. Vinodgopal, B. Neppolian, Influence of electron storing, transferring and shuttling assets of reduced graphene oxide at the interfacial copper doped TiO_2 p-n heterojunction for the increased hydrogen production, Nanoscale 7 (2015) 7849–7857.

[41] S.G. Babu, R. Vinoth, P.S. Narayana, D. Bahnemann, B. Neppolian, Reduced graphene oxide wrapped Cu_2O supported on C_3N_4: an efficient visible light responsive semiconductor photocatalyst, APL Mater. 3 (2015) 104415–104418.